

Targeting Androgen Receptor in Estrogen Receptor-Negative Breast Cancer

Min Ni,^{1,4} Yiwen Chen,^{2,4} Elgene Lim,¹ Hallie Wimberly,³ Shannon T. Bailey,¹ Yuuki Imai,¹ David L. Rimm,³ X. Shirley Liu,^{2,*} and Myles Brown^{1,*}

¹Division of Molecular and Cellular Oncology, Department of Medical Oncology, Dana-Farber Cancer Institute and Department of Medicine, Brigham and Women's Hospital and Harvard Medical School

²Department of Biostatistics and Computational Biology, Dana-Farber Cancer Institute and Harvard School of Public Health Boston, MA 02215, USA

³Department of Pathology, Yale University School of Medicine, New Haven, CT 06520, USA

⁴These authors contributed equally to this work

*Correspondence: xslu@jimmy.harvard.edu (X.S.L.), myles_brown@dfci.harvard.edu (M.B.)

DOI 10.1016/j.ccr.2011.05.026

SUMMARY

Endocrine therapies for breast cancer that target the estrogen receptor (ER) are ineffective in the 25%–30% of cases that are ER negative (ER⁻). Androgen receptor (AR) is expressed in 60%–70% of breast tumors, independent of ER status. How androgens and AR regulate breast cancer growth remains largely unknown. We find that AR is enriched in ER⁻ breast tumors that overexpress HER2. Through analysis of the AR cistrome and androgen-regulated gene expression in ER⁻/HER2⁺ breast cancers we find that AR mediates ligand-dependent activation of Wnt and HER2 signaling pathways through direct transcriptional induction of WNT7B and HER3. Specific targeting of AR, Wnt or HER2 signaling impairs androgen-stimulated tumor cell growth suggesting potential therapeutic approaches for ER⁻/HER2⁺ breast cancers.

INTRODUCTION

Sex steroid hormones are critical for the development and progression of cancers of reproductive organs including the uterus and breast in women and the prostate in men. Although estrogen is considered to be a female-selective sex steroid and androgen a male one, both are present and play important developmental functions in both sexes. Whereas estrogen is widely recognized for its role in breast cancer, little is known concerning a potential role for androgen in this disease. Steroid hormone receptors are crucial components of steroid hormone signaling that act as transcription factors to regulate gene expression; however, their function contributes to hormonal carcinogenesis. Studies of estrogen and estrogen receptor (ER) have led to significant progress in the development of endocrine therapies targeting estrogen production or ER for both breast cancer treatment and prevention. However, there are

currently no effective endocrine therapies for the 25%–30% of breast cancers that are ER-negative (ER⁻).

In addition to defining breast cancers based on their expression of ER, the recognition of the role played by amplification of the HER2 oncogene has had a major impact on the disease. Therapies targeting HER2 such as trastuzumab are becoming increasingly important in the treatment of HER2⁺ tumors of all stages. Nonetheless, despite endocrine therapies for ER⁺ tumors and HER2-targeted therapies for HER2⁺ tumors, significant numbers of breast tumors fail to respond. Recent studies have found that the androgen receptor (AR) is expressed in 60%–70% of breast cancers regardless of ER status (Agoff et al., 2003; Kuenen-Boumeester et al., 1996; Niemeier et al., 2010). It has been postulated that AR functions as an anti-proliferative effector in ER⁺ breast cancer by antagonizing ER (Peters et al., 2009), whereas it facilitates tumor cell growth in an androgen-dependent manner in an ER⁻/AR⁺ breast cancer cell

Significance

Endocrine therapies that target the estrogen receptor (ER) are the cornerstone of breast cancer treatment for the majority of patients. However, 25%–30% of breast tumors do not express ER and are not responsive to existing endocrine therapies. The androgen receptor (AR) is also expressed in a majority of breast tumors, even in those that lack ER. By coupling ChIP-seq technology with genome-wide analysis of gene expression, we have identified a previously unappreciated function of AR in regulating oncogenic Wnt and HER2 signaling in breast cancer leading to androgen-stimulated growth of ER⁻/HER2⁺ breast cancers. Our findings provide evidence that drugs targeting AR and the AR-regulated signaling cascade are potential therapies for ER-negative breast cancers harboring HER2 overexpression.

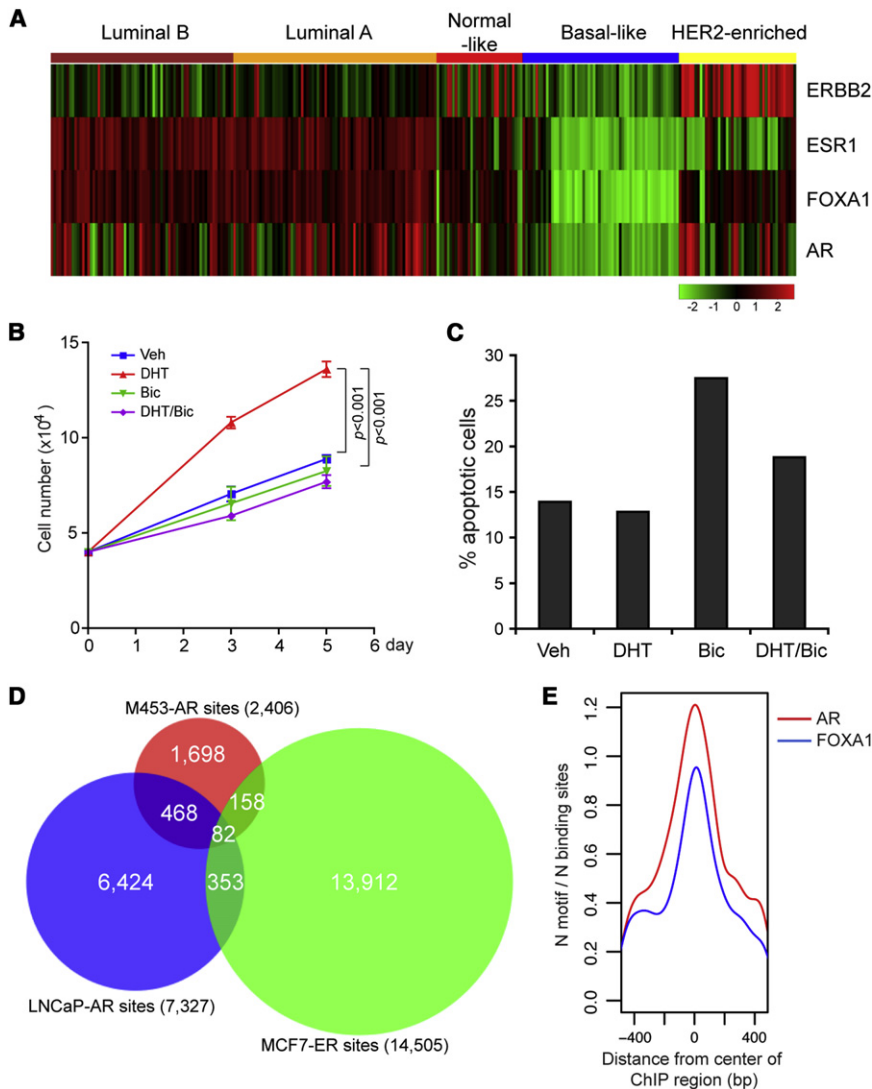


Figure 1. Androgen Receptor Is Functionally Active in ER-/HER2+ Breast Cancer

(A) Heatmap of a breast cancer microarray data set (Wang et al., 2005a) showing the expression levels of *ERBB2/HER2*, *ESR1*, *AR*, and *FOXA1* across the five breast cancer subtypes classified by the PAM50 gene signature. The AR expression is highly correlated with HER2 status of ER-breast tumors ($r_{\text{Pearson}} > 0.69$, $p < 6.6 \times 10^{-11}$).

(B) DHT stimulates the growth of MDA-MB-453 breast cancer cells and the AR antagonist bicalutamide (Bic) abrogates this effect. Data represent means \pm standard deviation (SD) from three independent replicates. Unpaired two-tail t test was used to examine the statistical difference and *p*-values are shown.

(C) Annexin-V apoptosis assay detects increased apoptosis induced by bicalutamide (Bic) in MDA-MB-453 breast cancer cells.

(D) Venn diagram showing the overlap between AR cistromes from MDA-MB-453 breast cancer cells and LNCaP prostate cancer cells (Wang et al., 2009) together with the ER cistrome from MCF7 breast cancer cells (Ross-Innes et al., 2010).

(E) Enrichment for the AR and FOXA1 binding motifs in the center of the AR binding sites specific to MDA-MB-453 cells. The occurrence of the motifs (N motifs) was normalized to the number of sites of the AR cistrome (N binding sites). See also Figure S1.

line model (Doane et al., 2006). The ER-/AR+ subclass was previously identified as a group of breast tumors with histological apocrine features and termed the molecular apocrine subtype (Farmer et al., 2005). Microarray analyses reveal intact and active AR signaling in ER-/AR+ breast tumors (Doane et al., 2006). However, the mechanism by which AR contributes to breast cancer development and progression is unknown. To comprehensively decipher the role of AR in breast cancer, we used an integrative analysis of the AR cistrome together with androgen-regulated gene expression profiles to define the important AR regulated pathways that are involved in stimulating the growth of ER-/HER2+ breast cancers.

RESULTS

AR Collaborates with FOXA1 in Global Transcriptional Activation of Androgen-Regulated Genes

Gene expression microarray studies provide an important tool for tumor classification, prognosis and as a guide to therapy.

into five subclasses (Luminal A, Luminal B, normal-like, basal-like, and HER2-enriched) and the gene expression level of AR together with the important biomarkers, ER, FOXA1, and HER2, are summarized in a heatmap (Figure 1A). Interestingly, we observed a high level of AR expression in HER2-enriched tumors. Importantly, within ER-negative subgroup that contains both basal-like and ER-/HER2+ tumors, high AR expression is correlated with HER2 amplification and overexpression ($r_{\text{Pearson}} > 0.69$, $p < 6.6 \times 10^{-11}$). Consistent with this observation, recent immunohistochemical studies also suggested a significant correlation of AR with HER2 overexpression in ER-negative breast tumors (Agoff et al., 2003; Niemeier et al., 2010; Park et al., 2010). Notably AR is not highly expressed in the basal-like subtype.

To understand the genomic action of androgens and AR in ER-/HER2+ breast cancer, we investigated the gene expression profiles of MDA-MB-453 human breast cancer cells treated with 5 α -dihydrotestosterone (DHT). This ER-/HER2+ breast cancer cell line belongs to HER2-enriched subtype based on the

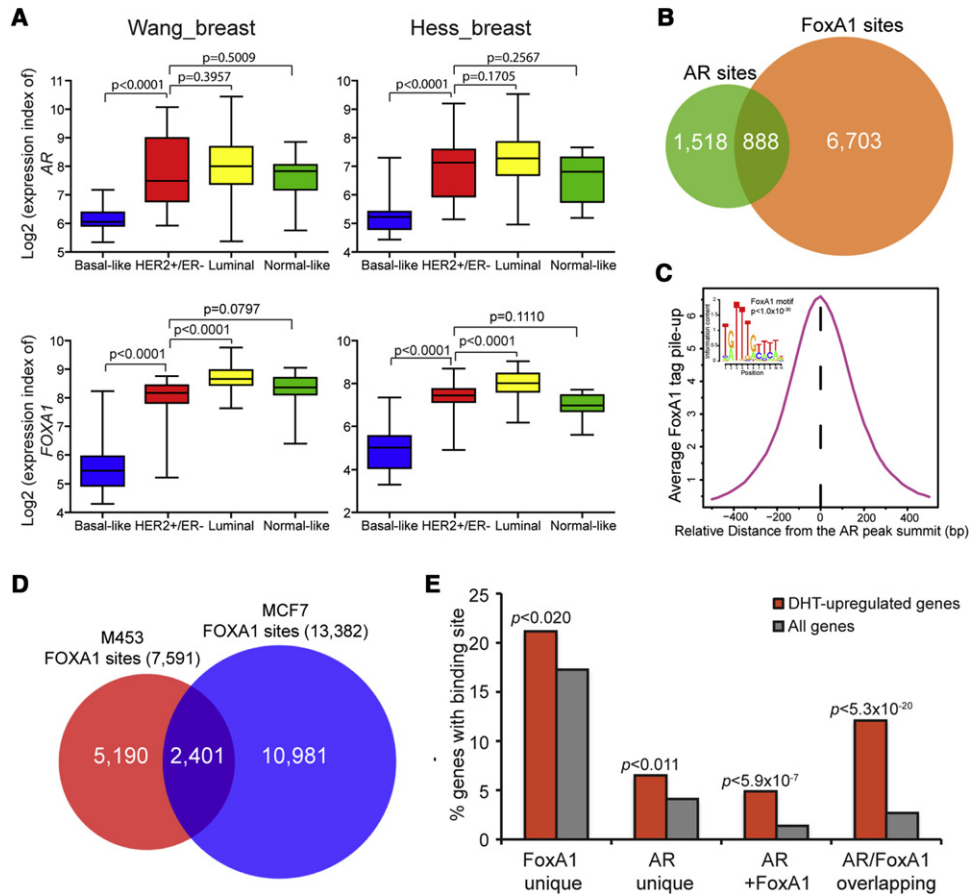


Figure 2. FOXA1 Collaborates with AR in Control of DHT Signaling in ER-/HER2+ Breast Cancer

(A) Comparison of AR and FOXA1 expression between ER-/HER2+ and basal-like, luminal or normal-like breast cancer subtypes using published microarray data sets (Hess et al., 2006; Wang et al., 2005a). Unpaired two-tail t test is used for p value calculation. The FOXA1 expression is highly correlated with AR levels within ER- breast tumors ($r_{\text{Pearson}} > 0.76$, $p < 2 \times 10^{-10}$).

(B) Venn diagram of the overlap between AR and FOXA1 cistromes.

(C) Sitepro analysis (Shin et al., 2009) of the genome-wide correlation between AR and FOXA1 binding sites. The average ChIP-seq signal is shown for the 1-kb region surrounding the center of AR binding sites.

(D) Venn diagram showing the overlap between hormone-stimulated FOXA1 cistromes from MDA-MB-453 and MCF7 (Eeckhoutte et al., 2009) breast cancer cells.

(E) Correlation between DHT-upregulated gene expression and binding of AR only (AR unique), FOXA1 only (FOXA1 unique), the two factors at non-overlapped but nearby sites (AR+FOXA1), and the two factors at the overlapped sites (AR/FOXA1 overlapping), within 50 kb of the TSS of genes. p values are shown.

See also Figure S2.

PAM50 gene signature. With abundant expression of AR (Doane et al., 2006), MDA-MB-453 cells showed increased growth responsiveness to androgens, such as DHT (Figure 1B) and the synthetic androgen R1881 (Doane et al., 2006). Addition of bicalutamide, a nonsteroidal AR antagonist, abolished the DHT-stimulated cell growth (Figure 1B) and also induced apoptosis (Figure 1C) in MDA-MB-453 breast cancer cells. Gene expression microarray analyses identified a total of 1341 genes that are differentially regulated by DHT (q-value ≤ 0.05 and fold change ≥ 1.5).

To identify the direct targets of AR transcriptional regulation, we performed AR chromatin immunoprecipitation followed by next-generation sequencing (ChIP-seq) to define the AR cistrome in MDA-MB-453 breast cancer cells. We identified a total of 2406 high-confidence AR binding sites after 4 hr of androgen stimulation ($p \leq 1 \times 10^{-5}$). These AR binding sites were found

predominantly at distal intergenic and intronic regions (see Figure S1A available online) and possessed highly conserved genomic sequences (Figure S1B). Interestingly, whereas this AR cistrome overlaps to a small degree with the AR cistrome in LNCaP prostate cancer cells or the ER cistrome in MCF7 ER+ breast cancer cells, the majority of the binding sites are cell-specific (Figure 1D). Thus, our study reveals a unique hormone-regulated AR cistrome in ER-/HER2+ breast cancer cells. Importantly, motif enrichment analysis of the AR cistrome revealed the presence of not only AR and other nuclear receptor binding motifs, but also forkhead factor binding motifs including FOXA1 (Figure 1E). Among all forkhead family transcription factors, FOXA1 is highly expressed in HER2+ breast tumors and associated with AR expression ($r_{\text{Pearson}} > 0.76$, $p < 2 \times 10^{-10}$), as compared to basal-like tumors of the ER-negative subgroup (Figures 1A and 2A). It is worth noting that high levels

of FOXA1 have been observed in AR+ prostate cancers (Mirosevich et al., 2006) and ER+ breast cancers (Lacroix and Leclercq, 2004). In addition to its expression in breast cancer, FOXA1 has been shown to maintain ER expression during normal mammary ductal morphogenesis (Bernardo et al., 2010) and to act as a cell-type specific pioneer factor that facilitates recruitment of ER and AR to their *cis*-regulatory elements across the genome (Lupien et al., 2008). To gain further insight into the potential association between FOXA1 and AR in ER-/HER2+ breast cancer, we determined the FOXA1 cistrome in MDA-MB-453 cells and identified 7591 high-confidence FOXA1 binding sites ($p \leq 1 \times 10^{-5}$). We observed a significant overlap (~37%) between the AR and FOXA1 cistromes in MDA-MB-453 breast cancer cells (Figure 2B). Analysis of ChIP-seq signals further verified a strong correlation and mutual enrichment between AR and FOXA1 binding (Figure 2C). Similar to the FOXA1 cistromes previously identified in MCF7 and LNCaP cells, the FOXA1 cistrome of MDA-MB-453 cells showed predominant enrichment in distal intergenic and intronic regulatory regions in genome (Figure S1C). These FOXA1 binding sites were highly conserved (Figure S1D) and significantly enriched with the FOXA1 binding motif (Figure 2C, inset). Interestingly, we observed a significant overlap of FOXA1 cistromes between MDA-MB-453 and MCF7 breast cancer cells (Figure 2D), however the overlapped AR/FOXA1 sites in MDA-MB-453 are largely distinct from the ER/FOXA1 sites in MCF7.

To determine the functional significance of AR and FOXA1 chromatin colocalization, we examined the correlation of transcription factor binding to DHT-regulated gene expression in MDA-MB-453 breast cancer cells. The sequences of overlapped AR/FOXA1 sites are highly conserved (Figure S2A) and overall either AR or FOXA1 binding sites are significantly enriched within 50 kb of transcriptional start sites (TSS) of the DHT-upregulated genes (Figures S2B–S2D). This was especially true for sites where AR and FOXA1 bound near to one another (Figure 2E). In contrast, the genes downregulated by DHT have only FOXA1 and not AR binding sites nearby (Figures S2C and S2D), suggesting a role of FOXA1 in maintaining basal expression of these genes and predominantly indirect mechanisms of androgen-mediated repression in this cell type (Lupien et al., 2008). These data indicate an important collaboration between AR and FOXA1 in transcriptional activation of AR target genes and androgen signaling in ER-/HER2+ breast cancer cells.

AR Activates Wnt/ β -Catenin Pathway through Transcriptional Upregulation of *WNT7B*

In keeping with the finding that AR showed cell-type-specific chromatin occupancy in breast cancer and prostate cancer cells in response to androgen stimulation, it also regulated distinct transcriptional programs. By defining the DHT-upregulated transcriptional program in MDA-MB-453 breast cancer cells, we found this gene signature was significantly correlated with the published overexpression gene signatures of HER2+ breast tumors and as well as ER+ breast tumors (Figure 3A) using OncoPrint Concepts Map analysis (Rhodes et al., 2007). In order to determine the identity of androgen-modulated biological pathways in MDA-MB-453 cells we performed gene set enrichment analysis (GSEA) (Subramanian et al., 2005) of the androgen-regulated genes. Among the highest scoring cate-

gories for the DHT-stimulated genes (Figure S3), we observed significant enrichment of genes in the Wnt signaling pathway (Figure 3B). Screening of the genes in the Wnt pathway overexpressed in MDA-MB-453 cells revealed the significant upregulation of the canonical Wnt ligand *WNT7B* (Figure 3C). Analysis of the AR cistrome identified an AR binding site within the *WNT7B* gene locus (+1.5 kb of TSS) (Figure 4A). We validated using ChIP-qPCR that the occupancy of AR at this site was enriched only after DHT stimulation in MDA-MB-453 cells (Figure 4B). We also confirmed by RT-PCR that DHT treatment substantially elevated the mRNA level of *WNT7B* (Figure 4C), and silencing of AR effectively impeded this induction (Figure S4A). The androgen-dependent upregulation of *WNT7B* by AR was further validated in two other ER- breast cancer cell lines HCC202 and SUM185PE, both of which express AR and showed increased growth responsiveness to androgen stimulation (Figure S4). These data suggest that AR directly activates *WNT7B* transcription in a ligand-dependent manner.

Wnt ligands are involved in the development of normal mammary gland and increased expression of *WNT1* is oncogenic in breast cancer models in mice (Turashvili et al., 2006). *WNT7B* acts in the canonical Wnt pathway and is expressed during the stages of ductal formation and involution in mammary gland development (Gavin and McMahon, 1992). *WNT7B* has the ability to maintain mammary epithelial cells in an uncommitted state (Weber-Hall et al., 1994) and its elevated expression has been found in 10% of all breast carcinomas (Huguet et al., 1994). We found by analyzing published breast tumor microarray data sets (Hess et al., 2006; Ivshina et al., 2006) that *WNT7B* expression is highly correlated with AR status ($r_{\text{Pearson}} > 0.44$, $p < 9 \times 10^{-3}$). As a canonical Wnt ligand, *WNT7B* activates TCF-regulated gene transcription in a cell-type-specific manner through the stabilization of β -catenin (Wang et al., 2005b). Interestingly, we found that DHT stimulation led to nuclear AR, increased *WNT7B* protein levels and the activation of β -catenin in MDA-MB-453 breast cancer cells, as demonstrated by the increased protein levels of β -catenin and its active form in the nuclear fraction (Figure 4D). Consistent with canonical Wnt signaling β -catenin mRNA levels were not affected (Figure S4B). To confirm whether the nuclear translocation of β -catenin is dependent on AR-mediated *WNT7B* upregulation, we transduced the MDA-MB-453 cells with lentiviral shRNA targeting either *WNT7B* or *AR* and the subcellular localization of β -catenin was determined by confocal microscopy. As shown in Figure 4E, DHT treatment induced the nuclear accumulation of both β -catenin and AR. In contrast, silencing of *WNT7B* or *AR* significantly abrogated β -catenin nuclear localization (Figure 4E), indicating that AR and *WNT7B* mediate Wnt/ β -catenin activation in response to DHT.

β -Catenin Cooperates with AR in Transcriptional Upregulation of *HER3*

In the canonical Wnt pathway, nuclear β -catenin is a pivotal regulator of TCF-regulated gene transcription. β -catenin has also been shown to act as a coregulator of AR in prostate cancer cells to enhance the transcriptional activity of AR (Yang et al., 2002). We detected the physical interaction between AR and β -catenin in the nuclear extracts of MDA-MB-453 breast cancer cells by coimmunoprecipitation (Figure 5A). However, neither

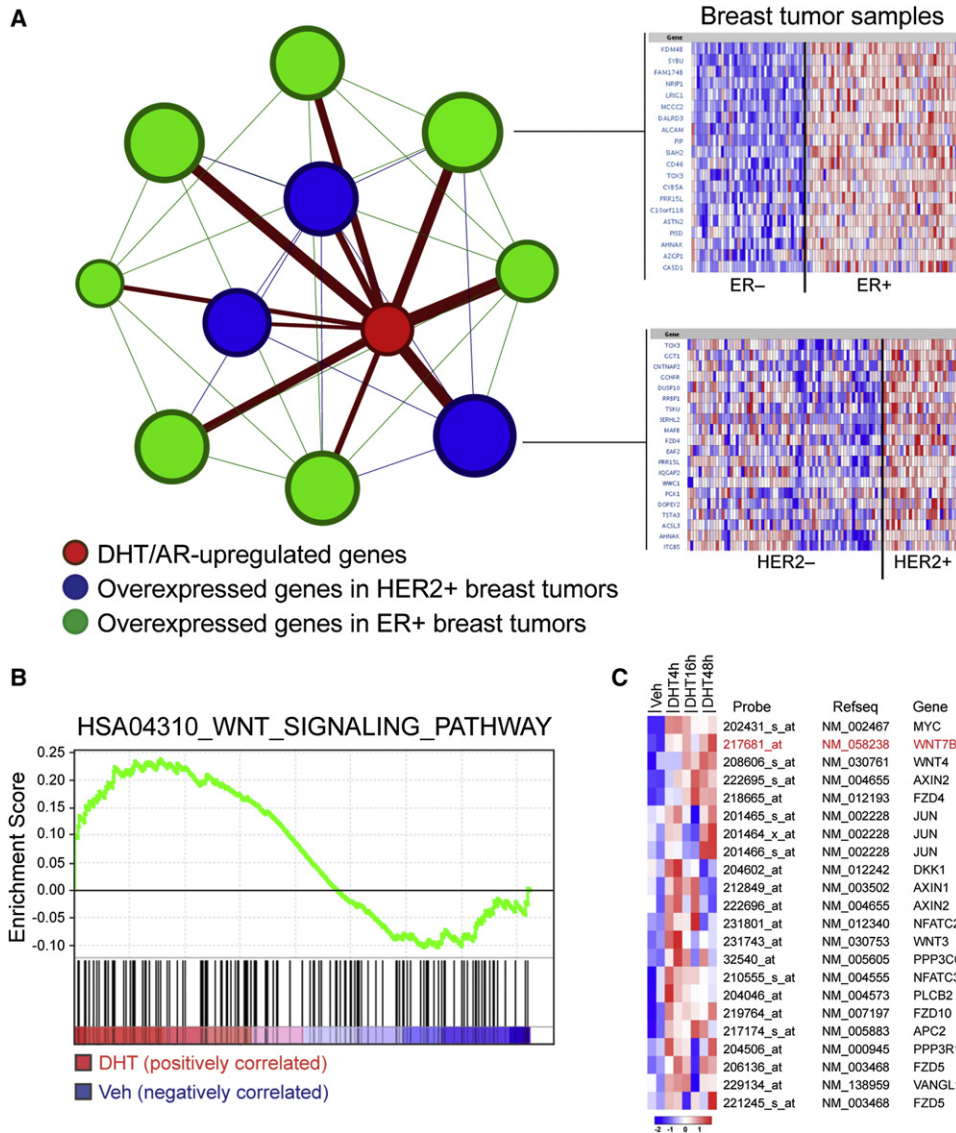


Figure 3. Characterization of DHT-Induced Gene Signature in ER-/HER2+ Breast Cancer Cells

(A) OncoPrint Concepts Map analysis (Compendia Biosciences) was used to compare the DHT/AR-induced gene signature in MDA-MB-453 cells against all published gene signatures from primary breast tumors, and reveals statistically significant correlations between DHT-induced genes specifically associated with AR binding sites within 50 kb of their TSS and gene expression signatures of HER2+ breast tumors as well as ER+ breast tumors. (Left) The association between molecular concepts of different gene signatures or gene sets is represented as a graph using Gephi (<http://gephi.org>), in which a node represents a gene set and significantly associated sets ($q \leq 2.3 \times 10^{-4}$) were connected by an edge. The node of AR-upregulated gene set was colored in red, and the nodes of overexpression gene sets from HER2+ or ER+ breast tumors were colored in blue and green, respectively. The thickness of the edges that connect the node of AR-upregulated gene set with other nodes is proportional to the rank of the association significance. The size of a node is proportional to the number of overlapping genes between its corresponding gene sets and AR-upregulated gene set. The right panel presents examples of the significant correlation between the DHT/AR-induced gene signature with the published ER+ breast cancer gene signature and HER2+ breast cancer gene signature established in two independent studies (Minn et al., 2005; Lu et al., 2008).

(B) Plot from gene set enrichment analysis (GSEA) (Subramanian et al., 2005) showing enrichment of the Wnt pathway in DHT-upregulated transcription program.

(C) Gene expression microarray heatmap showing the DHT-induced expression of genes involved in the Wnt signaling pathway.

See also Figure S3.

DHT nor recombinant WNT7B protein was able to activate the TCF/LEF TOP-Flash reporter; instead they suppressed the luciferase activity and the cotreatment displayed a synergistic inhibitory effect (Figure S5A). This inhibition is likely due to a previously described mechanism in prostate cancer in which AR competes with TCFs for limiting amounts of nuclear β -catenin, thus sup-

pressing β -catenin/TCF transcriptional activity (Chesire and Isaacs, 2002; Mulholland et al., 2003). Moreover, DHT treatment led to decreased expression of the four TCF/LEF family genes (Figure S5B) in MDA-MB-453 breast cancer cells, suggesting an additional mechanism by which androgen and AR inhibit TCF-regulated transcription.

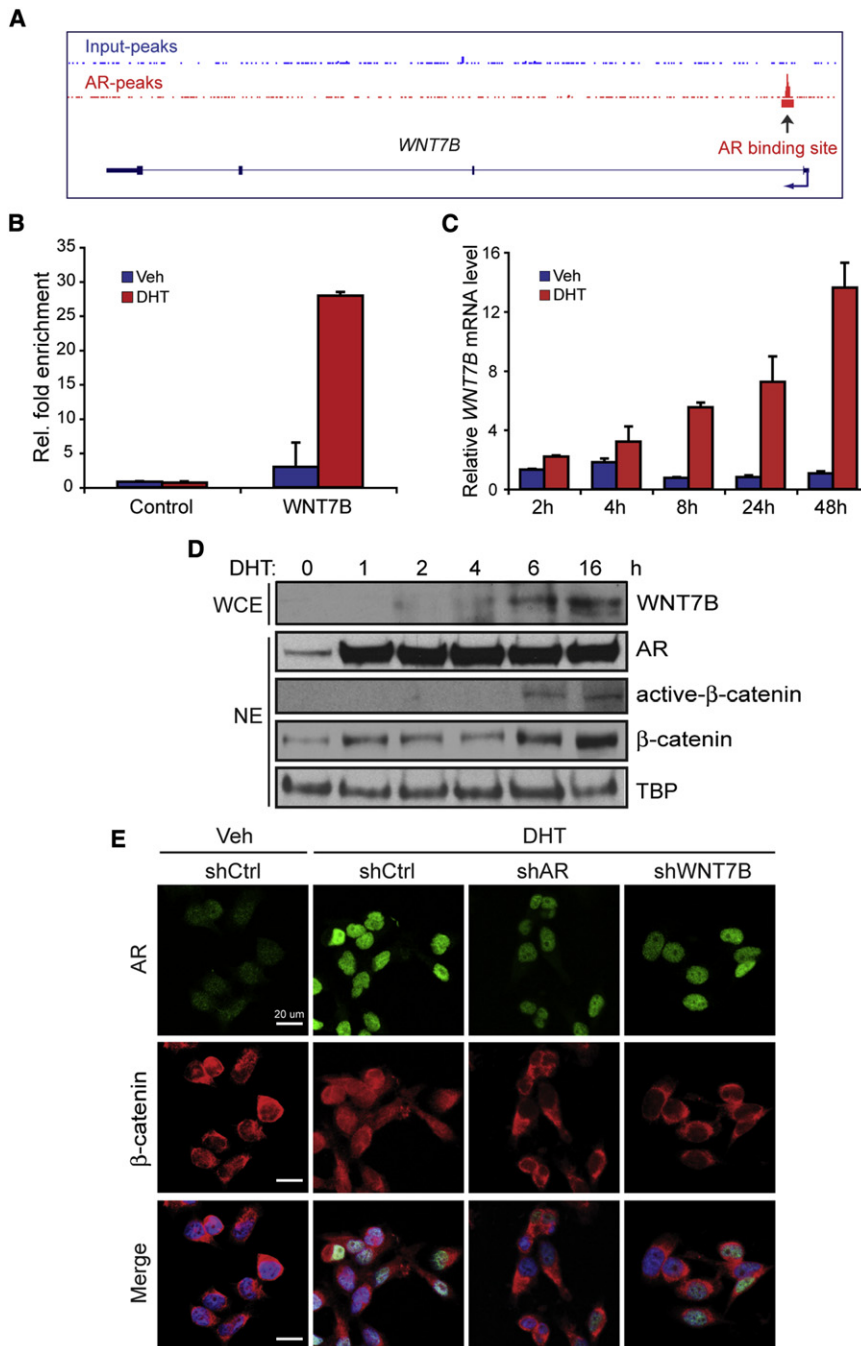


Figure 4. AR-Mediated Transcriptional Up-regulation of WNT7B Activates β-Catenin

(A) Schematic diagram of the AR binding site within the *WNT7B* gene locus (+1.5 kb of TSS) as defined by AR ChIP-seq.

(B) Direct AR ChIP followed by quantitative PCR after treatment with vehicle (blue bars) or 10 nM DHT (red bars) for 4 hr in MDA-MB-453 breast cancer cells. Primers flanking GAPDH promoter region were used as a control. Data represent means with SD.

(C) *WNT7B* mRNA level was determined by real-time RT-PCR after MDA-MB-453 cells were treated with vehicle (blue bars) or 10 nM DHT (red bars) for the indicated times. mRNA levels are presented as means with SD.

(D) Whole cellular extracts (WCE) or nuclear extracts (NE) from vehicle or DHT-treated MDA-MB-453 cells were subjected to immunoblotting for the indicated proteins.

(E) Confocal immunofluorescence microscopy showing endogenous AR (green) and β-catenin (red) in lentiviral shRNA-transfected MDA-MB-453 cells after treatment with vehicle (Veh) or 10 nM DHT for 3 days in hormone-depleted medium. DAPI staining indicates the nucleus. Scale bars represent 20 μM.

See also Figure S4.

intergenic and intronic regions and are highly enriched near the DHT-upregulated genes (Figure 5B). Analysis of the 4 hr-AR, 16 hr-AR, and FOXA1 cistromes revealed significant numbers of sites that were differentially occupied by AR at 4 hr and 16 hr of DHT treatment (Figure 5C). There was significant overlap between AR at both time points with FOXA1. The differential androgen-stimulated AR binding patterns at early and late time points suggested a hierarchical regulatory network involving AR, FOXA1, and other AR cofactors. To investigate the potential targets regulated by AR and β-catenin, we first examined the overlapped sites between 16 hr-AR and FOXA1 (744 sites as shown in Figure 5C) and the nearby genes. Interestingly, gene ontology (GO) analysis revealed that genes with uniquely overlapped 16 hr-AR/FOXA1 binding sites within 50 kb of their TSS were significantly associated with several important biological processes including most notably “regulation of cell proliferation” (Figure 5D). Through screening of the genes involved in these GO categories, we found *HER3* as a gene involved in several of the enriched biological processes (Figure 5D, highlighted in red). Inspection of the FOXA1 and 16 hr-AR cistromes identified a site bound by both close to the TSS of the *HER3* gene (Figure 6A). We focused on *HER3* as it encodes an important coreceptor of HER2 in HER2+ breast cancers. We demonstrated that FOXA1 binding at the *HER3* gene was dramatically increased after DHT treatment, and

Physical interaction between AR and β-catenin represents a secondary response to androgen stimulation. Their interaction has been previously implicated in prostate cancer progression (Mulholland et al., 2005; Terry et al., 2006). However, the genes coregulated by AR and β-catenin are not known. To investigate the regulatory role of AR in collaboration with β-catenin, we defined the AR cistrome at a late time point (16 hr) after prolonged DHT stimulation. AR ChIP-seq revealed a total of 3431 high-confidence sites in MDA-MB-453 cells ($p \leq 1 \times 10^{-5}$). Similar to the 4 hr-AR cistrome, these 16 hr-AR sites are mainly located in distal

associated with several important biological processes including most notably “regulation of cell proliferation” (Figure 5D). Through screening of the genes involved in these GO categories, we found *HER3* as a gene involved in several of the enriched biological processes (Figure 5D, highlighted in red). Inspection of the FOXA1 and 16 hr-AR cistromes identified a site bound by both close to the TSS of the *HER3* gene (Figure 6A). We focused on *HER3* as it encodes an important coreceptor of HER2 in HER2+ breast cancers. We demonstrated that FOXA1 binding at the *HER3* gene was dramatically increased after DHT treatment, and

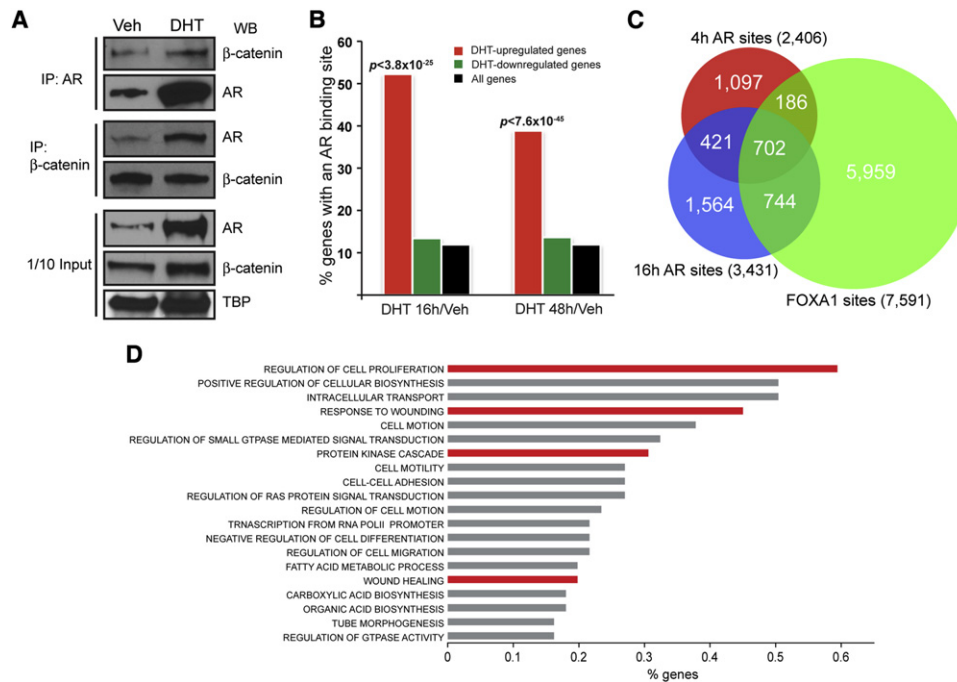


Figure 5. Prolonged DHT-Stimulation Leads to a Distinct AR Cistrome in ER⁻/HER2⁺ Breast Cancer Cells

(A) Coimmunoprecipitation of endogenous AR and β-catenin from the nuclear extracts of MDA-MB-453 breast cancer cells after 4 hr stimulation with vehicle (Veh) or 10 nM DHT.

(B) Correlation between DHT-regulated genes and 16 hr-AR cistrome in MDA-MB-453 breast cancer cells.

(C) Venn diagram showing the overlap between AR and FOXA1 cistromes in MDA-MB-453 breast cancer cells.

(D) Functional annotation of the genes that uniquely possess overlapped 16 hr-AR and FOXA1 binding sites. Top overrepresented gene categories ($p \leq 0.05$) from gene ontology (GO) biological process are shown and the categories involving *HER3* are colored in red.

concomitantly, a substantially enhanced occupancy of both AR and β-catenin was also verified at this same region in MDA-MB-453 (Figure 6B) and as well SUM185PE breast cancer cells (Figure S5E).

Sequence analysis of this overlapped AR/FOXA1 region revealed two FOXA1 binding motifs and one ARE half-site motif nearby (Figure S5C). Additionally, three TCF4/TCF7L2 motifs also occur within this 950-bp region (Figure S5C, blue boxes). Given that TCF factors recruit β-catenin to chromatin as part of canonical Wnt signaling and DHT downregulates TCF expression in MDA-MB-453 breast cancer cells, we speculated that TCF4 might initially reside at this regulatory region of the *HER3* gene before AR activation, and may recruit β-catenin together with AR on DHT stimulation. Consistent with this hypothesis, TCF4 ChIP showed that TCF4 was able to occupy the same region in the absence of DHT, whereas the recruitment of TCF4 to *HER3* gradually declined after DHT stimulation (Figure S5D), likely due to the DHT-mediated downregulation of TCFs in MDA-MB-453 cells as described above. Androgen stimulation led to increased expression of *HER3*, which was abrogated by silencing of AR or β-catenin (Figures 6C and 6D). As expected, AR silencing caused a decrease in β-catenin at protein levels; interestingly, β-catenin knockdown also diminished AR expression in MDA-MB-453 cells (Figure 6D). This observation implicated a feedback mechanism between Wnt/β-catenin and androgen/AR pathways. In prostate cancer cells, it has been suggested that Wnt signaling modulates AR transcriptional

activity and protein stability by multiple pathways (reviewed in Terry et al., 2006), including direct regulation of AR transcription and protein stability by β-catenin/TCF (Yang et al., 2006). These findings indicate a regulatory mechanism by which androgen induces *HER3* expression in ER⁻/HER2⁺ breast cancer cells through collaboration between AR and β-catenin.

HER3 together with EGFR/HER1, HER2, and HER4 constitutes the HER family of tyrosine kinases. It is through dimerization and transphosphorylation that the HER members trigger signaling cascades. Importantly, HER2 activation requires heterodimerization with another HER receptor due to its lack of ligand binding activity (Baselga and Swain, 2009). The significance of HER3 in HER2⁺ breast tumors is well recognized for its ability to form heterodimers with HER2 and modulate the PI3K/AKT pathway (reviewed in Baselga and Swain, 2009). HER3 is thought to be an important determinant of the oncogenic activity of HER2 in breast cancer (Hsieh and Moasser, 2007; Lee-Hoeflich et al., 2008). It has been shown that increased HER3 expression substantially augments HER2 signaling, and contributes to the incomplete inhibition of HER2 activity by tyrosine kinase inhibitors (Sergina et al., 2007). Similarly, we observed that the phosphorylation of both HER3 and HER2 was elevated as an indication of the active HER2 signaling pathway during DHT treatment (Figure 6E). As a downstream event of HER2/HER3 signaling, the PI3K/AKT pathway was also significantly activated in response to androgen, demonstrated by the increased phosphorylation of AKT

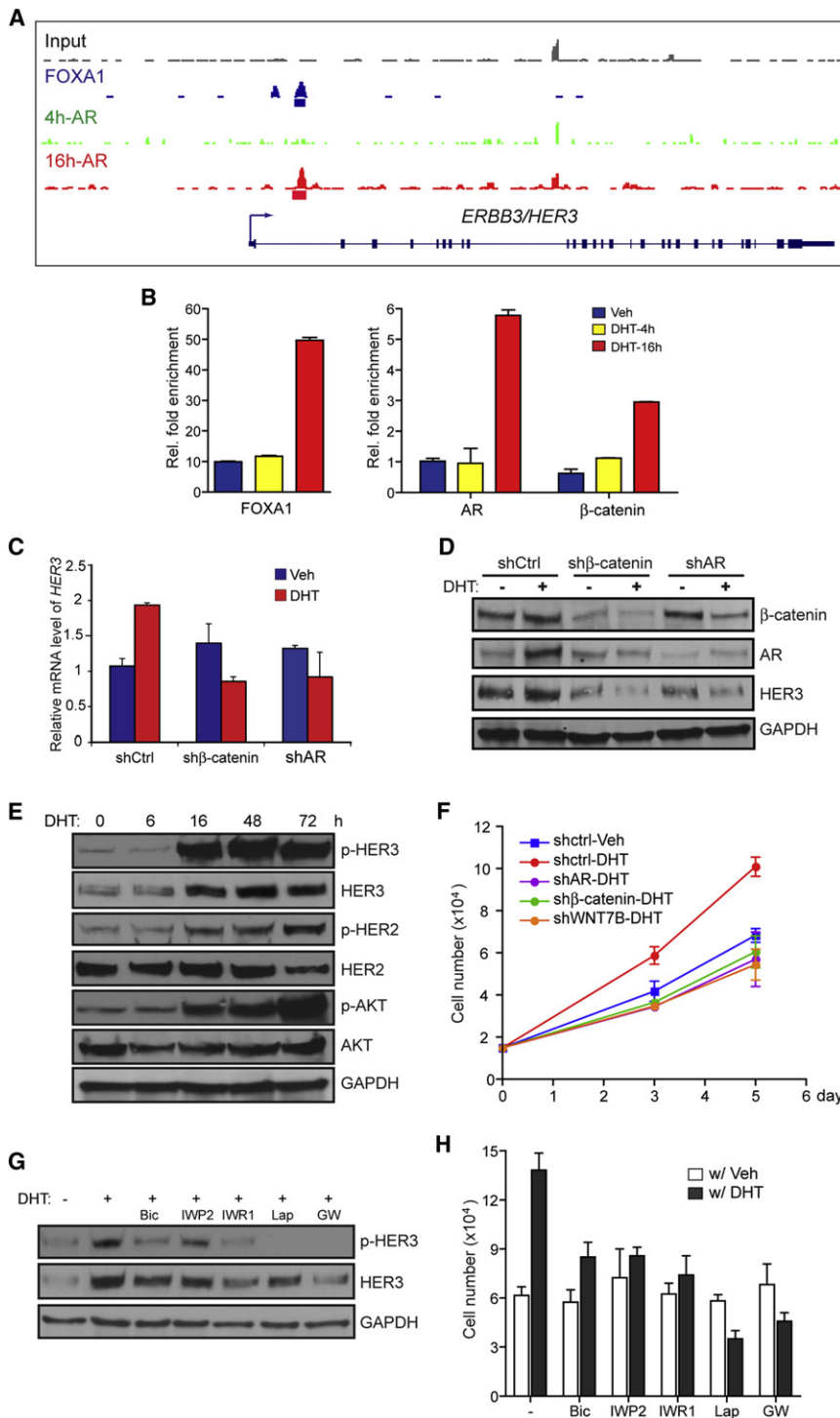


Figure 6. AR-Regulated HER3 Induction Activates HER2/HER3 Signaling Pathway in ER-/HER2+ Breast Cancer Cells

(A) Schematic representation showing the overlapped AR and FOXA1 binding site within the HER3 gene locus as defined by ChIP-seq in MDA-MB-453 breast cancer cells.

(B) Recruitment of FOXA1, AR, and β -catenin to the regulatory region of HER3 (+1.8 kb of TSS). Direct ChIP-qPCR of FOXA1, AR and β -catenin was performed to monitor their binding at HER3 gene after MDA-MB-453 cells were treated with vehicle or 10 nM DHT for 4 hr or 16 hr. Data represent means with SD.

(C) MDA-MB-453 cells transduced with the indicated shRNA lentivirus were treated with vehicle or DHT for 16 hr, and the total RNA was subjected to real-time RT-PCR of HER3. mRNA levels are presented as means with SD.

(D) Immunoblotting to determine HER3 expression in MDA-MB-453 cells after transduction of the indicated lentiviral shRNA followed by vehicle (-) or DHT (+) treatment for 16 hr in hormone-depleted medium.

(E) MDA-MB-453 breast cancer cells were treated with 10 nM DHT for the indicated times and assayed for expression and phosphorylation of the indicated proteins.

(F) Lentiviral shRNA-transduced MDA-MB-453 cells were cultured in hormone-depleted medium for 2 days followed by treatment with vehicle (Veh) or 10 nM DHT for the indicated time points, and the total numbers of viable cells were determined. The results are shown as means \pm SD from three independent replicates.

(G) MDA-MB-453 cells were treated with the indicated agents for 48 hr and HER3 and HER3 phosphorylation were measured by immunoblotting.

(H) After treatment with the indicated inhibitors in the presence of vehicle or 10 nM DHT for 3 days, the total numbers of viable cells were determined and the means from three independent replicates are shown with SD.

See also Figure S5.

(Figure 6E) in MDA-MB-453 cells. Activation of this signaling cascade was also observed in DHT-stimulated SUM185PE breast cancer cells (Figure S5F). These observations indicate that the elevated expression of HER3 in response to androgen leads to enforced HER2/HER3 signaling in ER-/HER2+ breast cancer cells.

of AR, WNT7B or β -catenin effectively impeded the DHT-induced cell growth (Figure 6F), confirming the important function of AR and WNT7B/ β -catenin in ER-/HER2+ breast cancer. To gain further insights into the effects of antagonizing AR and the AR-regulated signaling cascade in ER-/HER2+ breast cancer, we tested the pharmacological inhibitors targeting AR

Targeting Androgen-Induced HER2/HER3 Activation Impairs Tumor Cell Growth

HER3-mediated PI3K/AKT activation is crucial for maintaining cell proliferation and survival. Thus, we hypothesized that AR/ β -catenin-mediated upregulation of HER3 and activation of HER2/HER3 signaling might account for increased cell growth after androgen stimulation.

Consistent with this hypothesis, silencing

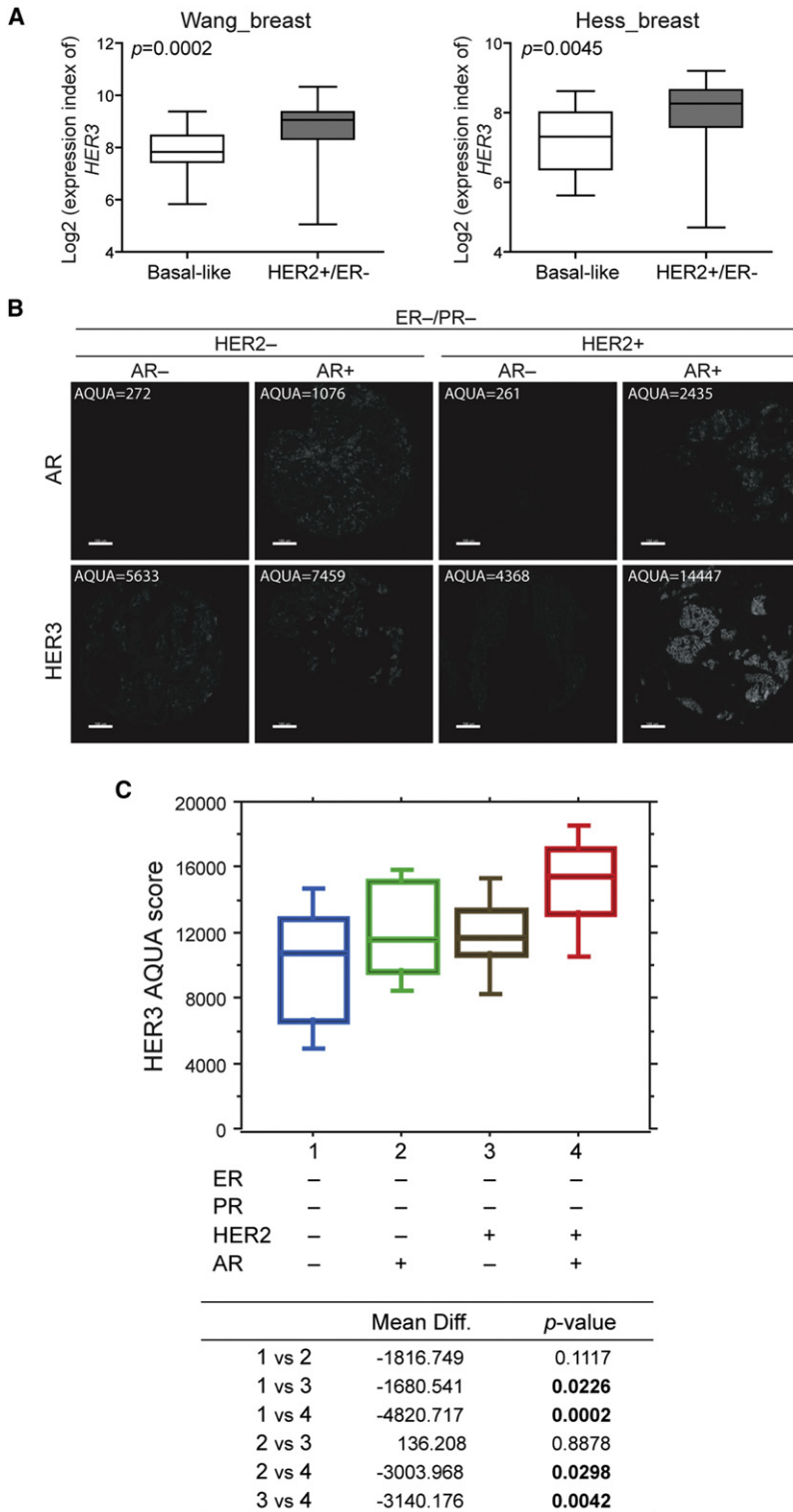


Figure 7. Coexpression of AR and HER3 in ER-/HER2+ Breast Tumors

(A) Comparison of *HER3* expression between ER-/HER2+ and basal-like breast cancer subtypes using published microarray data sets (Hess et al., 2006; Wang et al., 2005a). Unpaired two-tail t test is used for p value calculation. The *HER3* expression is highly correlated with AR levels of ER-/HER2+ tumors ($r_{\text{Pearson}} > 0.41$, $p < 2.8 \times 10^{-4}$).

(B) Representative AQUA output images of tissue microarray staining analysis for the four subtypes of ER-/PR- breast tumors based on AR (cutpoint >800) and HER2 status. AQUA scores are shown and the scale bars represent 100 μM .

(C) Quantitation of *HER3* staining in the four subtypes, HER2-/AR- (n = 93), HER2-/AR+ (n = 12), HER2+/AR- (n = 32) and HER2+/AR+ (n = 10) of ER-/PR- breast tumor samples by AQUA. p values were based on two-sided testing, and $p < 0.05$ was considered as statistically significant.

which blocked induction of *HER3* at mRNA level (Figure S5I). We further demonstrated that these inhibitors targeting AR, Wnt, or HER2 signaling greatly diminished DHT-induced *HER3* activation, shown as a decrease of both total protein level and phosphorylation of *HER3* in the presence of DHT (Figure 6G). In accordance with attenuated *HER3* activity, DHT-induced cell growth of MDA-MB-453 was abrogated by addition of these inhibitors (Figure 6H). Similar effects were observed in SUM185PE breast cancer cells (Figure S5G). Notably, the tyrosine kinase inhibitors, lapatinib and GW583340, were able to inhibit tumor cell growth significantly only with DHT cotreatment. This suggests that androgen stimulation increases the dependence on HER2/*HER3* signaling for growth in ER-/HER2+ breast tumors that express AR.

High Level of HER3 Is Correlated with AR Expression in ER-/HER2+ Breast Tumors

Using breast cancer cell lines, we identified *HER3* as a downstream target of AR. To determine whether *HER3* is also highly expressed in clinical ER-/HER2+ breast tumors, we first analyzed the published gene expression microarrays of breast tumor samples. Analysis of two independent data sets revealed significantly higher levels of *HER3* expression in ER-/HER2+ breast tumors compared to basal-like ones (Figure 7A) and importantly *HER3* expression is highly correlated with AR expression across all ER-negative breast tumors ($r_{\text{Pearson}} > 0.41$, $p < 2.8 \times 10^{-4}$). To further confirm this correlation, we performed immunohistochemical staining of AR and *HER3* in breast carcinoma tissue microarrays and quantified the levels of AR and *HER3* proteins in human breast cancer tissues by automated

(bicalutamide), Wnt/ β -catenin (IWP2 and IWR1) (Chen et al., 2009), or HER2 (tyrosine kinase inhibitors lapatinib and GW583340) in cell growth assays. Inhibitors targeting AR and Wnt/ β -catenin pathways were able to abolish the DHT-induced recruitment of AR and β -catenin to the *HER3* gene (Figure S5H),

which blocked induction of *HER3* at mRNA level (Figure S5I). We further demonstrated that these inhibitors targeting AR, Wnt, or HER2 signaling greatly diminished DHT-induced *HER3* activation, shown as a decrease of both total protein level and phosphorylation of *HER3* in the presence of DHT (Figure 6G). In accordance with attenuated *HER3* activity, DHT-induced cell growth of MDA-MB-453 was abrogated by addition of these inhibitors (Figure 6H). Similar effects were observed in SUM185PE breast cancer cells (Figure S5G). Notably, the tyrosine kinase inhibitors, lapatinib and GW583340, were able to inhibit tumor cell growth significantly only with DHT cotreatment. This suggests that androgen stimulation increases the dependence on HER2/*HER3* signaling for growth in ER-/HER2+ breast tumors that express AR.

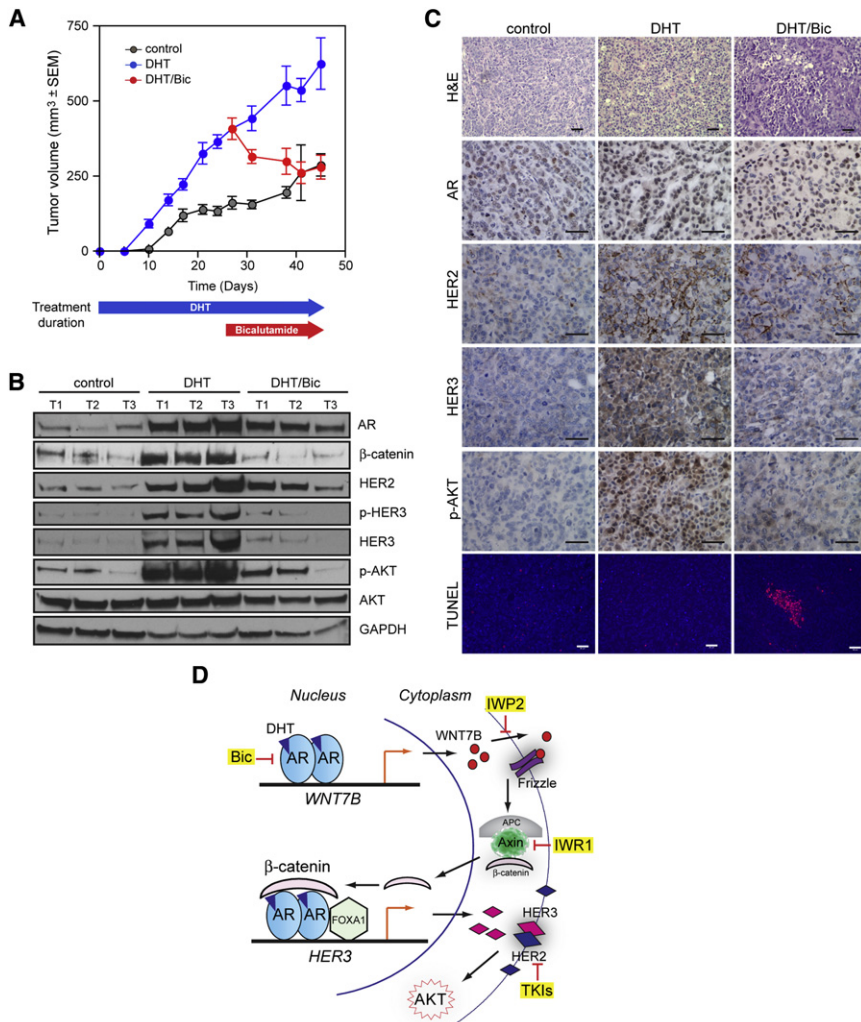


Figure 8. Bicalutamide Impedes DHT-Induced Tumor Growth In Vivo

(A) Effects of DHT and bicalutamide on the growth of MDA-MB-453 xenograft tumors. MDA-MB-453 cells were orthotopically implanted in the fourth inguinal gland of female NOD/SCID mice and the DHT release pellets were implanted subcutaneously at the same time in the surgery. Animals bearing tumors (>400 mm³ in size) were randomly grouped (8–10 mice/group) and treated with daily oral gavage of vehicle or bicalutamide (10 mg/kg) for 3 weeks. Data are presented as mean tumor volume ± SEM.

(B) Immunoblot analysis of MDA-MB-453 xenograft tumors from different treatment groups to examine the expression or phosphorylation of the indicated proteins. The whole cell extracts subjected to immunoblotting were prepared from three tumor samples for each group that were collected from three mice, respectively.

(C) The paraffin-embedded tumor sections were subjected to histological analysis by hematoxylin and eosin staining, immunohistochemical staining of the indicated proteins and TUNEL assays for in situ cell death detection. Scale bars represent 50 μM.

(D) Model of the regulatory role of AR in activating WNT7B/β-catenin and HER2/HER3 in ER–/HER2+ breast cancer. The inhibitors targeting AR, Wnt, or HER2 pathways are highlighted in yellow.

quantitative analysis (AQUA) (Camp et al., 2002). Figure 7B shows representative images from immunofluorescent labeling of AR and HER3 in four subtypes of ER–/PR– breast tumors classified by the expression of HER2 and AR. Each panel shows the AQUA score indicating the protein level of AR or HER3. AR expression is predominantly nuclear and HER3 expression was both membranous and cytoplasmic, notably excluded from the nuclear compartment (non-nuclear). The quantitative analysis demonstrated significantly higher HER3 expression in HER2+/AR+ breast tumors as compared to the other ER–/PR– subtypes (Figure 7C). Thus these analyses in breast cancer patient samples demonstrate that HER3 expression is correlated with AR and HER2 status in ER-negative breast cancers and support our finding that HER3 is a direct AR target.

Bicalutamide Inhibits the Growth of DHT-Stimulated ER–/HER2+ Breast Tumors In Vivo

To determine the antitumor effect of targeting AR in vivo, we established an MDA-MB-453 xenograft model. The MDA-MB-453 cells were implanted in the mammary gland of NOD/SCID mice, and one group of the mice received the concomitant implantation of a DHT slow-release pellet. DHT dramatically promoted

the growth of MDA-MB-453 tumors in vivo ($p = 0.0003$) (Figure 8A). After tumors reached a volume of 400 mm³, daily oral administration of bicalutamide at 10 mg/kg was delivered to 50% of the mice carrying DHT pellets ($n = 8$). As expected bicalutamide treatment resulted in a significant inhibition of DHT-stimulated growth of MDA-MB-453 xenograft tumors ($p = 0.0007$) and tumors regressed to control levels after 3 weeks of treatment (Figure 8A).

Immunoblot analysis of MDA-MB-453 tumor extracts confirmed that AR levels were elevated by DHT treatment in vivo. Consistent with our cell culture findings, the AR-regulated Wnt/β-catenin and HER2/HER3 signaling pathways were substantially induced in the tumors from the mice carrying DHT pellets, whereas bicalutamide treatment abrogated the DHT-induced activation of these pathways (Figure 8B). Hematoxylin and eosin staining of paraffin-embedded tumor sections revealed that whereas MDA-MB-453 xenografts exhibited well-organized sheets of round and cohesive undifferentiated tumor cells, the tumors treated with bicalutamide showed more discohesive cells within a disordered structure (Figure 8C). Tumor sections from each treatment group were further analyzed by immunohistochemical staining of AR and its targets to determine the effects of DHT and bicalutamide on their expression in vivo. Importantly, the DHT-treated xenograft tumors showed significant nuclear AR and membranous HER2 staining, and elevated HER3 and p-AKT levels as compared to the tumors from the mice without DHT pellets. Significantly, bicalutamide treatment

led to substantial reduction in expression of HER3 and p-AKT, and enhanced cell death as detected by TUNEL assay (Figure 8C). Taken together, these results demonstrate that inhibiting AR with bicalutamide blocked androgen-stimulated oncogenic HER2/HER3 signaling and inhibited the growth of ER⁻/HER2⁺/AR⁺ breast tumors in vivo.

DISCUSSION

Endocrine therapies that target estrogen and ER signaling pathways play a critical role in the treatment of the majority of breast cancer patients. However, over a quarter of breast tumors fail to express ER and are thus resistant to these therapies. Our findings suggest that there are a significant number of ER⁻/HER2⁺ breast tumors that express AR and are growth stimulated by androgens. We have shown that androgens and AR stimulate oncogenic Wnt and HER2 signaling pathways by transcriptional upregulation of *WNT7B* and *HER3* in ER⁻/HER2⁺ breast cancer (as summarized in Figure 8D), by which androgen stimulates tumor cell growth. This regulatory network indicates an intrinsic link between AR and growth factor pathways in ER-negative breast cancer.

Hormonal regulation of Wnt expression has been suggested in mammary gland development, such as *WNT4* by progesterone (Briskin et al., 2000), and *WNT5B* and *WNT7B* by human chorionic gonadotropin (hCG) (Kuorelahti et al., 2007), whereas the direct effect of androgen and AR on *WNT* expression was previously unknown in the normal mammary gland or breast tumors. Overexpression of Wnt causes aberrant activation of the Wnt signaling pathway, which is a major driving force in a broad spectrum of human cancers. In this study, we have shown that AR-stimulated elevation of *WNT7B* leads to activated nuclear translocation of β -catenin. This in turn leads to β -catenin interaction with AR to induce *HER3* gene expression. These findings highlight a crucial androgen-dependent signaling cascade that is regulated by AR in ER⁻/HER2⁺ breast cancer. The nuclear localization of β -catenin is an important predictor of poor prognosis and outcome in colorectal cancer. However, the subcellular location of β -catenin has not been well investigated in breast cancer. We find that the collaboration between β -catenin and AR together with FOXA1 plays an important role in ER⁻/HER2⁺ breast tumors through binding to regulatory regions of the *HER3* gene.

HER3 is receiving increased attention as a therapeutic target in HER2⁺ breast cancers. Clinical studies of EGFR and HER2 antagonists suggest that HER2⁺ breast cancer is primarily driven by HER2/HER3 heterodimers rather than HER2/EGFR heterodimers (reviewed in Baselga and Swain [2009]). Interfering with HER2/HER3 heterodimerization has been suggested as an option to inhibit HER3 activation with the development of agents such as pertuzumab. Our work indicates that targeting AR with antagonists such as bicalutamide, may be another way to target HER3. Clinical trials of the anti-androgen bicalutamide in ER⁻/AR⁺ metastatic breast cancer are ongoing (NCT00468715). Our study also suggests that pharmacological inhibitors targeting AR-regulated pathways will only be effective in the presence of active androgen signaling and may be limited to ER⁻/HER2⁺ tumors. Expression of androgen/AR-regulated genes in ER⁻/HER2⁺ breast tumors could be predictors of a therapeutic

response to AR target therapies. It has been shown that the signaling pathways including Wnt, HER2 and PI3K/AKT are able to actively enforce AR activity, constituting positive feed-forward circuits (Mellinghoff et al., 2004; Mulholland et al., 2006; Terry et al., 2006). This may potentially lead to androgen-independent AR activation in breast tumors, as has been demonstrated in castration-resistant prostate cancer (Wang et al., 2009). Collectively, this work provides not only novel insights into androgen-dependent AR function in breast cancer, but also reveals the mechanistic basis for targeting AR as a therapeutic opportunity for patients with invasive ER⁻/HER2⁺ breast tumors.

EXPERIMENTAL PROCEDURES

Gene Expression Microarray Analysis

Hormone-depleted MDA-MB-453 cells were treated with vehicle or 10 nM DHT for 4, 16, or 48 hr, and the total RNA was isolated and hybridized to Affymetrix human U133 plus 2.0 expression array. All Gene expression microarray data were normalized and summarized using RMA (Irizarry et al., 2003). The differentially expressed genes between DHT and vehicle conditions were identified using SAM algorithm (Tusher et al., 2001) that is implemented in the MeV program (Saeed et al., 2006) ($q \leq 0.05$, fold change ≥ 1.5). The raw data of breast tumor microarray were obtained from previous publication (Hess et al., 2006; Ivshina et al., 2006; Wang et al., 2005a) and were normalized using RMA (Irizarry et al., 2003). The intrinsic subtype of individual breast tumor sample in clinical data sets was assigned using a 50-gene signature (PAM50) based on a supervised approach (Parker et al., 2009). The coexpression between AR and *HER2*, *FOXA1*, *HER3*, or *WNT7B* across breast tumor subtypes was characterized using Pearson correlation coefficient. The differentially expressed genes between different subtypes were identified using Welch's t test ($q \leq 0.05$).

ChIP and ChIP-Seq

ChIP was performed as previously described (Carroll et al., 2005) and the AR and FOXA1 ChIP-seq experiments were performed in hormone-depleted MDA-MB-453 cells with 10 nM DHT exposure. Briefly, $5\text{--}10 \times 10^6$ cells were cross-linked with 1% formaldehyde for 10 min at room temperature. Chromatin was sonicated in SDS lysis buffer to 300–500 bp. Antibodies were incubated with sonicated chromatin overnight, followed by incubation with Dynabead Protein A (Invitrogen) for 4 hr for chromatin collection. Concentrations of the ChIP DNA were quantified by Qubit Fluorometer (Invitrogen). Fifteen nanograms of the input (total sonicated chromatin DNA) or 6 ng of the ChIP samples were subjected to poly(A) tailing process (see Supplemental Experimental Procedures for details) and direct sequencing using Helicos HeliScope sequencer at Dana-Farber Cancer Institute. The antibodies used in ChIP experiments are AR (N-20, Santa Cruz), FOXA1 (ab-23738 from Abcam), β -catenin (H-102, Santa Cruz), and TCF4/TCF7L2 (N-20, Santa Cruz and clone6H5-3, Millipore).

Co-IP and Immunoblot Analysis

The endogenous co-IP experiments were performed using nuclear extracts as described previously (Xu et al., 2010). Briefly, 5 mg of nuclear extracts were incubated with 5 μ g of AR or β -catenin antibody on a rotator overnight at 4°C. The protein complexes were precipitated by addition of protein G/A-agarose beads (Roche) with incubation for 4 hr at 4°C. After wash for four times for 15 min, the beads were boiled for 5 min in protein sample buffer (Bio-Rad). The antibodies used for IP include AR (N-20, Santa Cruz) and β -catenin (H-102, Santa Cruz). The immunoprecipitated products or the cell lysates were processed for immunoblot as described previously (Wang et al., 2007) using antibodies against AR, HER3, TBP, and GAPDH from Santa Cruz, β -catenin and active β -catenin from Millipore, WNT7B from Novus, p-HER3, p-HER2, p-AKT, HER2, and AKT from Cell Signaling.

Immunohistochemical Staining and Automated Quantitative Analysis of Tissue Microarrays

The staining of AR and HER3 was performed on the archival Yale breast carcinoma tissue microarray cohort by a modified indirect immunofluorescence

method as described previously (Camp et al., 2002; Rubin et al., 2004). The tumor compartment of each histospot was defined using anticytokeratin antibodies and the primary antibodies are AR (Dako AR441), and HER3 (noncommercial antibody from CST, D11E5). Secondary labeling of targets was performed by signal amplification using horseradish peroxidase-labeled secondary reagents (species-specific Dako Envision) followed by Cy-5 tyramide incubation. DAPI in an anti-fading mounting medium was used for nuclear staining. Automated quantitative analysis (AQUA) is a method that allows exact and objective measurement of protein levels within a defined tumor area, as described previously (Camp et al., 2002). All statistical analysis was performed using Stat-View software and p values were based on two-sided testing, and $p < 0.05$ was considered as statistically significant. The tissue assessed in this study was obtained from the Yale Pathology Archives based on Yale Human Investigation Committee protocols #9505008219, #0304025173, and #0003011706. These protocols, to Dr. David Rimm, allow retrieval of tissue from archives that was consented or has been approved for use with waiver of consent.

Orthotopic Tumor Growth Assays

Six-week-old female NOD-SCID-IL2R γ C α −/− mice (Jackson Lab) were used for xenograft studies. Approximately 6×10^6 viable MDA-MB-453 cells were resuspended in 30 μ l 50% growth factor-reduced Matrigel (BD Biosciences) and injected orthotopically into the fourth inguinal gland as previously described (Torres-Arzuayus et al., 2006). The DHT release pellet (60 day release pellet, Innovative Research of America) was implanted subcutaneously at the time of surgery. The mice bearing tumors $>400 \text{ mm}^3$ were randomly grouped and treated by daily oral administration with vehicle or bicalutamide (10 mg/kg). Tumor volume was determined by measuring the minimum and maximum tumor diameters using the formula: $(\text{minimum diameter})^2 \times (\text{maximum diameter})/2$. All animal protocols were conducted with the approval of the IACUC at Dana-Farber Cancer Institute.

ACCESSION NUMBERS

Gene expression microarray and ChIP-seq data have been deposited in the Gene Expression Omnibus database with accession number GSE28789.

SUPPLEMENTAL INFORMATION

Supplemental Information includes five figures and Supplemental Experimental Procedures and can be found with this article online at doi:10.1016/j.ccr.2011.05.026.

ACKNOWLEDGMENTS

We are grateful to Cheng Fan, Joel Parker, Philip Bernard and Charles Perou for kindly sharing their data sets. We thank Yi Zheng and Xi Chen for technical support. We thank Michael Verzi, Thomas Westerling, Mathieu Lupien, and Jian Xu for helpful advice and discussions. This work was partly supported by a grant from the National Cancer Institute (P01CA080111 to M.B.), the National Institutes of Health (R01HG004069 to X.S.L.), and a Department of Defense Award (W81XWH-10-1-0037 to M.N.).

Received: September 15, 2010

Revised: March 28, 2011

Accepted: May 27, 2011

Published: July 11, 2011

REFERENCES

Agoff, S.N., Swanson, P.E., Linden, H., Hawes, S.E., and Lawton, T.J. (2003). Androgen receptor expression in estrogen receptor-negative breast cancer. Immunohistochemical, clinical, and prognostic associations. *Am. J. Clin. Pathol.* **120**, 725–731.

Baselga, J., and Swain, S.M. (2009). Novel anticancer targets: revisiting ERBB2 and discovering ERBB3. *Nat. Rev. Cancer* **9**, 463–475.

Bernardo, G.M., Lozada, K.L., Miedler, J.D., Harburg, G., Hewitt, S.C., Mosley, J.D., Godwin, A.K., Korach, K.S., Visvader, J.E., Kaestner, K.H., et al. (2010). FOXA1 is an essential determinant of ERalpha expression and mammary ductal morphogenesis. *Development* **137**, 2045–2054.

Briskin, C., Heineman, A., Chavarria, T., Elenbaas, B., Tan, J., Dey, S.K., McMahon, J.A., McMahon, A.P., and Weinberg, R.A. (2000). Essential function of Wnt-4 in mammary gland development downstream of progesterone signaling. *Genes Dev.* **14**, 650–654.

Camp, R.L., Chung, G.G., and Rimm, D.L. (2002). Automated subcellular localization and quantification of protein expression in tissue microarrays. *Nat. Med.* **8**, 1323–1327.

Carroll, J.S., Liu, X.S., Brodsky, A.S., Li, W., Meyer, C.A., Szary, A.J., Eeckhoutte, J., Shao, W., Hestermann, E.V., Geistlinger, T.R., et al. (2005). Chromosome-wide mapping of estrogen receptor binding reveals long-range regulation requiring the forkhead protein FoxA1. *Cell* **122**, 33–43.

Chen, B., Dodge, M.E., Tang, W., Lu, J., Ma, Z., Fan, C.W., Wei, S., Hao, W., Kilgore, J., Williams, N.S., et al. (2009). Small molecule-mediated disruption of Wnt-dependent signaling in tissue regeneration and cancer. *Nat. Chem. Biol.* **5**, 100–107.

Cheshire, D.R., and Isaacs, W.B. (2002). Ligand-dependent inhibition of beta-catenin/TCF signaling by androgen receptor. *Oncogene* **21**, 8453–8469.

Doane, A.S., Danso, M., Lal, P., Donaton, M., Zhang, L., Hudis, C., and Gerald, W.L. (2006). An estrogen receptor-negative breast cancer subset characterized by a hormonally regulated transcriptional program and response to androgen. *Oncogene* **25**, 3994–4008.

Eeckhoutte, J., Lupien, M., Meyer, C.A., Verzi, M.P., Shivdasani, R.A., Liu, X.S., and Brown, M. (2009). Cell-type selective chromatin remodeling defines the active subset of FOXA1-bound enhancers. *Genome Res.* **19**, 372–380.

Farmer, P., Bonnefoi, H., Becette, V., Tubiana-Hulin, M., Fumoleau, P., Larsimont, D., Macgrogan, G., Bergh, J., Cameron, D., Goldstein, D., et al. (2005). Identification of molecular apocrine breast tumours by microarray analysis. *Oncogene* **24**, 4660–4671.

Gavin, B.J., and McMahon, A.P. (1992). Differential regulation of the Wnt gene family during pregnancy and lactation suggests a role in postnatal development of the mammary gland. *Mol. Cell. Biol.* **12**, 2418–2423.

Hess, K.R., Anderson, K., Symmans, W.F., Valero, V., Ibrahim, N., Mejia, J.A., Booser, D., Theriault, R.L., Buzdar, A.U., Dempsey, P.J., et al. (2006). Pharmacogenomic predictor of sensitivity to preoperative chemotherapy with paclitaxel and fluorouracil, doxorubicin, and cyclophosphamide in breast cancer. *J. Clin. Oncol.* **24**, 4236–4244.

Hsieh, A.C., and Moasser, M.M. (2007). Targeting HER proteins in cancer therapy and the role of the non-target HER3. *Br. J. Cancer* **97**, 453–457.

Hu, Z., Fan, C., Oh, D.S., Marron, J.S., He, X., Qaqish, B.F., Livasy, C., Carey, L.A., Reynolds, E., Dressler, L., et al. (2006). The molecular portraits of breast tumors are conserved across microarray platforms. *BMC Genomics* **7**, 96.

Huguet, E.L., McMahon, J.A., McMahon, A.P., Bicknell, R., and Harris, A.L. (1994). Differential expression of human Wnt genes 2, 3, 4, and 7B in human breast cell lines and normal and disease states of human breast tissue. *Cancer Res.* **54**, 2615–2621.

Irizarry, R.A., Bolstad, B.M., Collin, F., Cope, L.M., Hobbs, B., and Speed, T.P. (2003). Summaries of Affymetrix GeneChip probe level data. *Nucleic Acids Res.* **31**, e15.

Ivshina, A.V., George, J., Senko, O., Mow, B., Putti, T.C., Smeds, J., Lindahl, T., Pawitan, Y., Hall, P., Nordgren, H., et al. (2006). Genetic reclassification of histologic grade delineates new clinical subtypes of breast cancer. *Cancer Res.* **66**, 10292–10301.

Kuonen-Boumeester, V., Van der Kwast, T.H., Claassen, C.C., Look, M.P., Liem, G.S., Klijn, J.G., and Henzen-Logmans, S.C. (1996). The clinical significance of androgen receptors in breast cancer and their relation to histological and cell biological parameters. *Eur. J. Cancer* **32A**, 1560–1565.

Kuorelahti, A., Rulli, S., Huhtaniemi, I., and Poutanen, M. (2007). Human chorionic gonadotropin (hCG) up-regulates wnt5b and wnt7b in the mammary gland, and hCGbeta transgenic female mice present with mammary Gland

- tumors exhibiting characteristics of the Wnt/beta-catenin pathway activation. *Endocrinology* 148, 3694–3703.
- Lacroix, M., and Leclercq, G. (2004). About GATA3, HNF3A, and XBP1, three genes co-expressed with the oestrogen receptor-alpha gene (ESR1) in breast cancer. *Mol. Cell. Endocrinol.* 219, 1–7.
- Lee-Hoeflich, S.T., Crocker, L., Yao, E., Pham, T., Munroe, X., Hoeflich, K.P., Sliwkowski, M.X., and Stern, H.M. (2008). A central role for HER3 in HER2-amplified breast cancer: implications for targeted therapy. *Cancer Res.* 68, 5878–5887.
- Lu, X., Wang, Z.C., Iglehart, J.D., Zhang, X., and Richardson, A.L. (2008). Predicting features of breast cancer with gene expression patterns. *Breast Cancer Res. Treat.* 108, 191–201.
- Lupien, M., Eeckhoutte, J., Meyer, C.A., Wang, Q., Zhang, Y., Li, W., Carroll, J.S., Liu, X.S., and Brown, M. (2008). FoxA1 translates epigenetic signatures into enhancer-driven lineage-specific transcription. *Cell* 132, 958–970.
- Mellinghoff, I.K., Vivanco, I., Kwon, A., Tran, C., Wongvipat, J., and Sawyers, C.L. (2004). HER2/neu kinase-dependent modulation of androgen receptor function through effects on DNA binding and stability. *Cancer Cell* 6, 517–527.
- Minn, A.J., Gupta, G.P., Siegel, P.M., Bos, P.D., Shu, W., Giri, D.D., Viale, A., Olshen, A.B., Gerald, W.L., and Massagué, J. (2005). Genes that mediate breast cancer metastasis to lung. *Nature* 436, 518–524.
- Mirosevich, J., Gao, N., Gupta, A., Shappell, S.B., Jove, R., and Matusik, R.J. (2006). Expression and role of Foxa proteins in prostate cancer. *Prostate* 66, 1013–1028.
- Mulholland, D.J., Read, J.T., Rennie, P.S., Cox, M.E., and Nelson, C.C. (2003). Functional localization and competition between the androgen receptor and T-cell factor for nuclear beta-catenin: a means for inhibition of the Tcf signaling axis. *Oncogene* 22, 5602–5613.
- Mulholland, D.J., Dedhar, S., Coetzee, G.A., and Nelson, C.C. (2005). Interaction of nuclear receptors with the Wnt/beta-catenin/Tcf signaling axis: Wnt you like to know? *Endocr. Rev.* 26, 898–915.
- Mulholland, D.J., Dedhar, S., Wu, H., and Nelson, C.C. (2006). PTEN and GSK3beta: key regulators of progression to androgen-independent prostate cancer. *Oncogene* 25, 329–337.
- Niemeier, L.A., Dabbs, D.J., Beriwal, S., Striebel, J.M., and Bhargava, R. (2010). Androgen receptor in breast cancer: expression in estrogen receptor-positive tumors and in estrogen receptor-negative tumors with apocrine differentiation. *Mod. Pathol.* 23, 205–212.
- Park, S., Koo, J., Park, H.S., Kim, J.H., Choi, S.Y., Lee, J.H., Park, B.W., and Lee, K.S. (2010). Expression of androgen receptors in primary breast cancer. *Ann. Oncol.* 21, 488–492.
- Parker, J.S., Mullins, M., Cheang, M.C., Leung, S., Voduc, D., Vickery, T., Davies, S., Fauron, C., He, X., Hu, Z., et al. (2009). Supervised risk predictor of breast cancer based on intrinsic subtypes. *J. Clin. Oncol.* 27, 1160–1167.
- Peters, A.A., Buchanan, G., Ricciardelli, C., Bianco-Miotto, T., Centenera, M.M., Harris, J.M., Jindal, S., Segara, D., Jia, L., Moore, N.L., et al. (2009). Androgen receptor inhibits estrogen receptor-alpha activity and is prognostic in breast cancer. *Cancer Res.* 69, 6131–6140.
- Rhodes, D.R., Kalyana-Sundaram, S., Tomlins, S.A., Mahavisno, V., Kasper, N., Varambally, R., Barrette, T.R., Ghosh, D., Varambally, S., and Chinnaiyan, A.M. (2007). Molecular concepts analysis links tumors, pathways, mechanisms, and drugs. *Neoplasia* 9, 443–454.
- Ross-Innes, C.S., Stark, R., Holmes, K.A., Schmidt, D., Spyrou, C., Russell, R., Massie, C.E., Vowler, S.L., Eldridge, M., and Carroll, J.S. (2010). Cooperative interaction between retinoic acid receptor-alpha and estrogen receptor in breast cancer. *Genes Dev.* 24, 171–182.
- Rubin, M.A., Zerkowski, M.P., Camp, R.L., Kuefer, R., Hofer, M.D., Chinnaiyan, A.M., and Rimm, D.L. (2004). Quantitative determination of expression of the prostate cancer protein alpha-methylacyl-CoA racemase using automated quantitative analysis (AQUA): a novel paradigm for automated and continuous biomarker measurements. *Am. J. Pathol.* 164, 831–840.
- Saeed, A.I., Bhagabati, N.K., Braisted, J.C., Liang, W., Sharov, V., Howe, E.A., Li, J., Thiagarajan, M., White, J.A., and Quackenbush, J. (2006). TM4 microarray software suite. *Methods Enzymol.* 411, 134–193.
- Sergina, N.V., Rausch, M., Wang, D., Blair, J., Hann, B., Shokat, K.M., and Moasser, M.M. (2007). Escape from HER-family tyrosine kinase inhibitor therapy by the kinase-inactive HER3. *Nature* 445, 437–441.
- Shin, H., Liu, T., Manrai, A.K., and Liu, X.S. (2009). CEAS: cis-regulatory element annotation system. *Bioinformatics* 25, 2605–2606.
- Sørlie, T., Perou, C.M., Tibshirani, R., Aas, T., Geisler, S., Johnsen, H., Hastie, T., Eisen, M.B., van de Rijn, M., Jeffrey, S.S., et al. (2001). Gene expression patterns of breast carcinomas distinguish tumor subclasses with clinical implications. *Proc. Natl. Acad. Sci. USA* 98, 10869–10874.
- Sørlie, T., Tibshirani, R., Parker, J., Hastie, T., Marron, J.S., Nobel, A., Deng, S., Johnsen, H., Pesich, R., Geisler, S., et al. (2003). Repeated observation of breast tumor subtypes in independent gene expression data sets. *Proc. Natl. Acad. Sci. USA* 100, 8418–8423.
- Subramanian, A., Tamayo, P., Mootha, V.K., Mukherjee, S., Ebert, B.L., Gillette, M.A., Paulovich, A., Pomeroy, S.L., Golub, T.R., Lander, E.S., and Mesirov, J.P. (2005). Gene set enrichment analysis: a knowledge-based approach for interpreting genome-wide expression profiles. *Proc. Natl. Acad. Sci. USA* 102, 15545–15550.
- Terry, S., Yang, X., Chen, M.W., Vacherot, F., and Buttyan, R. (2006). Multifaceted interaction between the androgen and Wnt signaling pathways and the implication for prostate cancer. *J. Cell. Biochem.* 99, 402–410.
- Torres-Arzayus, M.I., Yuan, J., DellaGatta, J.L., Lane, H., Kung, A.L., and Brown, M. (2006). Targeting the AIB1 oncogene through mammalian target of rapamycin inhibition in the mammary gland. *Cancer Res.* 66, 11381–11388.
- Turashvili, G., Bouchal, J., Burkadze, G., and Kolar, Z. (2006). Wnt signaling pathway in mammary gland development and carcinogenesis. *Pathobiology* 73, 213–223.
- Tusher, V.G., Tibshirani, R., and Chu, G. (2001). Significance analysis of microarrays applied to the ionizing radiation response. *Proc. Natl. Acad. Sci. USA* 98, 5116–5121.
- Wang, Y., Kljin, J.G., Zhang, Y., Sieuwerts, A.M., Look, M.P., Yang, F., Talantov, D., Timmermans, M., Meijer-van Gelder, M.E., Yu, J., et al. (2005a). Gene-expression profiles to predict distant metastasis of lymph-node-negative primary breast cancer. *Lancet* 365, 671–679.
- Wang, Z., Shu, W., Lu, M.M., and Morrisey, E.E. (2005b). Wnt7b activates canonical signaling in epithelial and vascular smooth muscle cells through interactions with Fzd1, Fzd10, and LRP5. *Mol. Cell. Biol.* 25, 5022–5030.
- Wang, Q., Li, W., Liu, X.S., Carroll, J.S., Jänne, O.A., Keeton, E.K., Chinnaiyan, A.M., Pienta, K.J., and Brown, M. (2007). A hierarchical network of transcription factors governs androgen receptor-dependent prostate cancer growth. *Mol. Cell* 27, 380–392.
- Wang, Q., Li, W., Zhang, Y., Yuan, X., Xu, K., Yu, J., Chen, Z., Beroukhim, R., Wang, H., Lupien, M., et al. (2009). Androgen receptor regulates a distinct transcription program in androgen-independent prostate cancer. *Cell* 138, 245–256.
- Weber-Hall, S.J., Phippard, D.J., Niemeier, C.C., and Dale, T.C. (1994). Developmental and hormonal regulation of Wnt gene expression in the mouse mammary gland. *Differentiation* 57, 205–214.
- Xu, J., Sankaran, V.G., Ni, M., Menne, T.F., Puram, R.V., Kim, W., and Orkin, S.H. (2010). Transcriptional silencing of gamma-globin by BCL11A involves long-range interactions and cooperation with SOX6. *Genes Dev.* 24, 783–798.
- Yang, F., Li, X., Sharma, M., Sasaki, C.Y., Longo, D.L., Lim, B., and Sun, Z. (2002). Linking beta-catenin to androgen-signaling pathway. *J. Biol. Chem.* 277, 11336–11344.
- Yang, X., Chen, M.W., Terry, S., Vacherot, F., Bemis, D.L., Capodice, J., Kitajewski, J., de la Taille, A., Benson, M.C., Guo, Y., and Buttyan, R. (2006). Complex regulation of human androgen receptor expression by Wnt signaling in prostate cancer cells. *Oncogene* 25, 3436–3444.